Variable Stiffness Hip Joint for Lower-limb Exoskeletons

Sophia Otálora[1], Hector A. Moreno[2], Marcela Múnera[3,4], and Carlos A. Cifuentes[3], *Senior Member*, IEEE

***Abstract*—The use of robotics in rehabilitation is a growing area of research, with the potential to greatly improve the quality of life for individuals with impairments. Robotic exoskeletons, in particular, have shown promise for enhancing mobility and independence in patients with conditions such as stroke. Current exoskeleton designs, however, often lack the necessary degrees of freedom (DOFs) to provide adequate balance and support during activities of daily living (ADLs), such as walking and standing. This study proposes a new lower limb exoskeleton design incorporating a variable stiffness hip joint based on a four-bar mechanism. This joint provides additional DOFs for improved balance and stability during gait, making it easier for patients to perform ADLs. The results show that the exoskeleton effectively improves stability during gait testing. This suggests that the proposed design can greatly enhance mobility and independence in impaired patients and could be a valuable tool in rehabilitation robotics.**

***Index Terms*—Passive joint, exoskeleton, mechanical design.**

I. INTRODUCTION

ROBOTIC devices have been widely used in gait rehabilitation as a tool for therapists and health care personnel, aimed at therapeutic and assistive tasks [1], [2]. They have been developed to reduce the burden of repetitive tasks and intensive training, allowing proper recovery for patients in conventional therapy [1]. Several devices have been deployed specifically for gait rehabilitation, divided into treadmill-based and overground exoskeletons [3]. These devices have been designed to assist according to a training scenario [4]. Over the years, a few devices have been underscored within clinical applications and research platforms such as Lokomat [5], LOPES [6], ALEX II [7], eLEGS [8], Indergo [9], ReWalk [10], Mindwalker [11], and HAL [12].

The lower-limb exoskeletons (LLE) previously mentioned have been designed in different configurations where they could allow one or more degrees of freedom (DOF) of the human joints (i.e., flexion/extension, ab/adduction, internal/external rotation); provide energy to the user's joints through an active or passive actuation system (i.e., electric, cable-driven, SEA, springs or dampers components); drive the user following a control system [2], [13]. According to these configurations, the exoskeleton provides multiple advantages and disadvantages for the user, such as back drivability, kinematic compatibility, comfort or discomfort, and heavy/lightweight device.

Each device made a trade-off between its targeted activity (e.g., walking, sit-to-stand, walking up/down stairs) and its configuration (i.e., overground or treadmill-based exoskeletons). For the hip ab/adduction, treadmill-based exoskeletons have actuators to provide energy to this motion, such as LOPES and ALEX II [6], [7]. In contrast to overground exoskeletons, which commonly restrict the hip ab/adduction motion. Within these devices are ReWalk, HAL, Indergo, and eLEGS [8]–[10], [12]. However, a few overground exoskeletons included compliant, quasi-passive or active hip joints along the frontal plane.

These devices intend to supply energy to the hip ab/adduction motion because of its importance along the gait, which could involve multiple measurements. For instance, the hip moment and hip power. Regarding gait, the hip extensor moment varies between 0.7 to -1.2 $Nm \cdot Kg^{-1}$, the hip abductor moment varies between -0.1 to 0.95 $Nm \cdot Kg^{-1}$, and the hip power fluctuates between -0.9 to 1.4 $W \cdot Kg^{-1}$ [14].

The designers provide multiple approaches to assist the hip ab/adduction motion to achieve the hip's kinetic requirements. For instance, Vanderbilt University's LLE has a compliant hip ab/ adduction frame using a composite material and aluminium inserts, increasing its weight [15]. However, these un-actuated joints have several limitations regarding the interaction torque delivered to the user, which depends on the frame's compliance. Exoskeletons with actuation in the frontal plane are essential for balance-related applications due to the active mediolateral stabilization in walking [16]. Also, hip torque is used in the frontal plane to counteract the momentum arising from gait perturbations, maintaining balance [17].

Other LLEs also included active and quasi-passive actuators to provide energy to the hip joint, even though these devices focus on the sagittal plane. Lee et al. studied a hip exoskeleton that provides an interaction maximum torque of 12 Nm through a 2.4 Kg structure [18]. Similarly, Di Natali et al. studied XoSoft, which uses quasi-passive actuators through elastic bands and an electro-magnetic clutch [19], [20]. This device generates passive energy along the motion, giving the user's hip a maximum torque of 3 Nm. Nevertheless, these kinetic outcomes are away from the hip's requirements.

Following the abovementioned context, this work proposes a passive joint for the hip ab/adduction motion to provide gait assistance, varying the interaction torque according to

[1]S. Otalora is with Graduate Program of Electrical Engineering, Federal University of Espirito Santo, Vitoria 29075-910, Brazil sophia.gonzalez@edu.ufes.br

[2]H. A. Moreno is with Facultad de Ingeniería Mecánica y Eléctrica, Universidad Autónoma de Coahuila, Av. Barranquilla s/n Col. Guadalupe, 25750, Monclova, Coah., Mexico h_moreno@uadec.edu.mx

[3]M. Munera and C. A. Cifuentes are with Bristol Robotics Laboratory, University of the West of England, Bristol, UK. marcela.munera@uwe.ac.uk, carlos.cifuentes@uwe.ac.uk

[4]M. Munera is with the Department of Biomedical Engineering, Colombian School of Engineering Julio Garavito, Bogota, Colombia

the user's needs. The joint is part of the AGoRA exoskeleton and is analyzed according to the mechanical structure shown in [21]. This joint is based on two design principles (i.e., variable stiffness system and a four-bar mechanism), explained in the next section. Besides, kinematic and static analysis are also established to relate these principles. Then, the analytical results are presented according to the pre-load of the system and the interaction torque. Finally, experimental results are shown to fully assess the purpose joint, analyzing the spatial-temporal parameters of ten subjects' gait.

II. Exoskeleton hip joint

The proposed passive hip joint is aimed to provide support along the frontal plane. The joint's design followed the joint's kinematic, which considered the range of motion (ROM) of the user's hip joint along the frontal plane mentioned in the previous section. As it is located in the frontal joint of the AGoRA LLE, the adjustable link varies the hip width, affecting the parameters of the joint (Fig. 1). Further analysis is performed through the torque interaction.

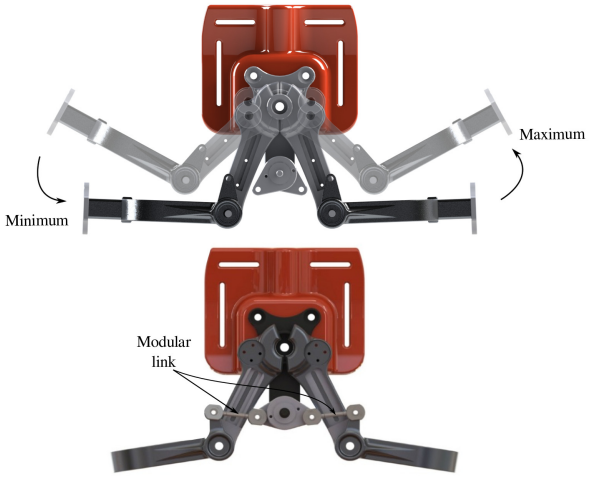

Fig. 1: Adjustable links of the AGoRA lower–limb exoskeleton along the frontal plane.

The joint combines three main design principles: variable stiffness principle, four-bar mechanism, and composite tendons. Each plays a role during the passive interaction between the user and the exoskeleton, providing an adjustable system to satisfy users' needs. Following these principles, the interaction torque is estimated through mathematical modelling to understand and quantify the energy and support deployed to the user.

A. Design principles

1) Four bar mechanism: Two double-rocker mechanisms are merged on the backside of the AGoRA LLE. Each mechanism is configured per side, as shown in Fig. 2. Focused on the right side of the exoskeleton, one of the rocker links directly interacts with the user's leg, and it pivots in O_2. Moreover, the opposite rocker pivoted in O_4 is loaded with the bio-inspired tendons' external forces.

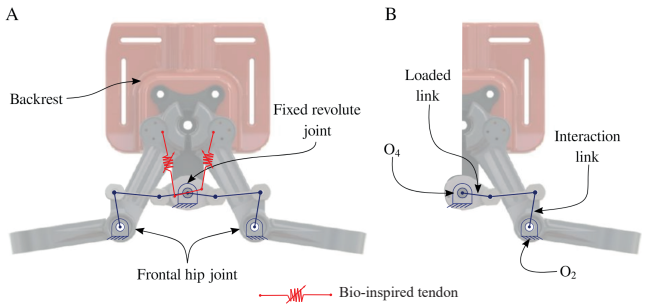

Fig. 2: Description of the passive frontal hip joint. A. Global overview of the passive frontal hip joint for both sides. B. Right-side description of the mechanism detailing the loaded and interaction links.

2) Variable stiffness tendons: The Variable Impedance Actuators (VIA) include active impedance control, inherent compliance, or inherent damping [22]. The passive actuators based on inherent compliance have intrinsic compliant elements that provide a fixed or variable stiffness due to their mechanical properties. According to these mechanical properties, they are divided into two categories: (1) Series Elastic Actuator (SEA) and (2) Variable Stiffness Actuator (VSA) [22]. However, the VIA could be delimited into many configurations regarding the mechanical interlink and the passive components (i.e., spring or damper). In this sense, the proposed passive joint is defined as a four-bar mechanism and a spring-like element previously described.

The passive elements involved in the VIA were designed to resemble the stiffness of a human tendon as a spring-like component. It was accomplished by a braided material formed by (1) an elastic filament (Filaflex, 2.85mm, Recreus, Spain) and (2) a fishing rod (eight filaments, Sufix 832, USA). These filaments were intertwined following a volumetric fraction of 14% to accomplish a variable stiffness performance regarding the elongation. A tensile test was conducted through a universal machine to assess this configuration, fixing a specimen between two jaws. Besides, the tensile tests followed the ASTM C1557-14 [23].

Stress-strain results estimate two elastic zones and Young's modulus, as shown in Fig. 3. A range of strain defines each zone: zone A is between 0 and 0.10 mm/mm, and zone B is between 0.1 and 0.15 mm/mm. Nevertheless, zone C presented inconsistent stress values and rupture points. However, this last zone is not considered in the analysis because the bio-inspired tendons will be loaded with forces smaller than the required for the rupture point.

III. METHODOLOGY

A. Kinematic and static analysis

Using the design principles, the kinematic and static analysis are presented in the following sections through an analytical approach based on Fig. 4.

1) Kinematic Analysis: From Fig. 4, it is possible to observe that the mechanism comprises two parts. The first part is a four-bar linkage; one of its links holds the user's femur. On the other hand, the central link is connected by a pair of tendons to support the mechanism.

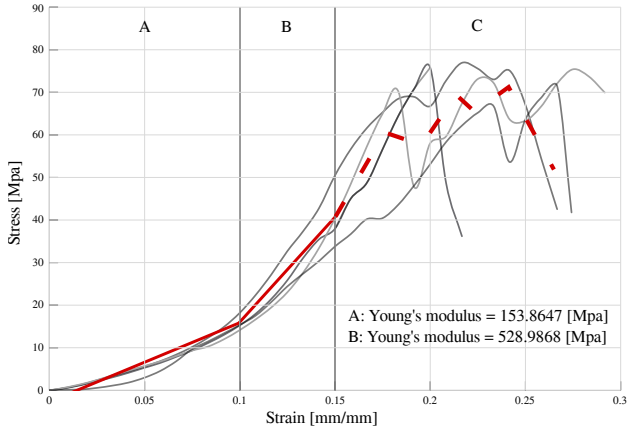

Fig. 3: Tensile results of the bio-inspired tendons. The stress-strain curve presents Young's modulus for the A and B zones.

From Fig. 4, it is possible to write the closed loop equation (Eq.1).

$$r_1 + r_2 - r_3 = s \tag{1}$$

given the orientation of r_3, expressed by angle θ_3, the orientation of the firs two links are obtained by Eq2

$$\theta_1 = 2\tan^{-1}\left(\frac{K_2 \pm \sqrt{K_1^2 + K_2^2 - Q_1^2}}{K_1 + Q_1}\right) \tag{2}$$

and, Eq. 3

$$\theta_2 = 2\tan^{-1}\left(\frac{K_2 \pm \sqrt{K_1^2 + K_2^2 - Q_2^2}}{K_1 + Q_2}\right) \tag{3}$$

where $K_1 = s_x + L_3\cos\theta_3$ and $K_2 = s_y + L_3\sin\theta_3$, $Q_1 = [L_1^2 - L_2^2 + K_1^2 + K_2^2]/2L_1$ and $Q_2 = [L_2^2 - L_1^2 + K_1^2 + K_2^2]/2L_2$, $L_1 = \|r_1\|$ is the length of the central link, $L_2 = \|r_2\|$ is the length of the rod, $L_3 = \|r_3\|$ is the length of the femur's link. Vector $s = \begin{bmatrix} s_x & s_y \end{bmatrix}^T$ defines the rotational joint of the femur's link.

On the other hand, for tendons, it is possible to write another closed loop equation, Eq. 4.

$$p_i - q_i - t_i = 0 \tag{4}$$

where $i \in \{r, l\}$. Given the orientation of the central link, expressed by angle θ_1, the length and orientation of the tendons can be obtained in Eq.5

$$t_i = \sqrt{p_{xi}^2 + p_{xi}^2 + q^2 - 2q[p_{xi}\cos(\theta_1 + \delta_i) + p_{yi}\sin(\theta_1 + \delta_i)]} \tag{5}$$

and, Eq.6

$$\rho = \tan^{-1}\left(\frac{p_{yi} - q\sin(\theta_1 + \delta_i)}{p_{xi} - q\cos(\theta_1 + \delta_i)}\right) \tag{6}$$

where vectors $p_i = \begin{bmatrix} p_{xi} & p_{yi} \end{bmatrix}^T$ and $q_i = q\begin{bmatrix} \cos(\theta_1 + \delta_i) & \cos(\theta_1 + \delta_i) \end{bmatrix}^T$ define the position of the anchor points of the tendons in the support and the central link, respectively.

2) Static Analysis: This analysis determines the expressions that relate the torque applied to the femur's subject and the force due to the extension of the tendons. In this analysis, the inertial forces are considered negligible because the mass of the links is small, and motion is performed at relatively slow velocities and accelerations. The torque applied to the femur is given by Eq.7.

$$\tau_D = \left(q_r^T \mathbf{K} f_r + q_l^T \mathbf{K} f_l\right) \frac{r_3^T \mathbf{K} \hat{r}_2}{r_1^T \mathbf{K} \hat{r}_2} \tag{7}$$

where f_r and f_l are the forces applied by the right and left tendons, respectively, $\hat{r}_2$ is the unit vector of r_2, and matrix $\mathbf{K}$ is given in Eq.8.

$$\mathbf{K} = \begin{bmatrix} 0 & -1 \\ 1 & 0 \end{bmatrix} \tag{8}$$

On the other hand, the internal forces applied at joints of the mechanism are described in Eq.9.

$$f_A = \|\left(\left(q_r^T \mathbf{K} f_r + q_l^T \mathbf{K} f_l\right)\hat{r}_2 / r_1^T \mathbf{K} \hat{r}_2 - f_r - f_l\right)\| \tag{9}$$

and, Eq.10

$$f_B = f_C = f_D = |\left(q_r^T \mathbf{K} f_r + q_l^T \mathbf{K} f_l\right)/r_1^T \mathbf{K} \hat{r}_2| \tag{10}$$

The previous expressions permit the determination of the forces generated in the mechanism for a given femur orientation concerning an initial configuration.

3) MATLAB modelling and simulations: Kinematic and static modelling are solved according to the hip ab/adduction ROM (i.e., 20°) to understand the passive frontal hip joint interaction. Following the analytical model previously mentioned, Algorithm 1 details the pseudo-code implemented in *Matlab R2018b* that estimates the torque interaction (i.e., τ_2). Three main functions are employed to estimate τ_2 divided into (1) *kinematic* and (2) *external forces*. According to the current parameters of the four-bar mechanism, τ_2 is estimated in different scenarios due to the variable stiffness configuration. These scenarios are delimited by the initial elongation, which can be adjusted in P_1 and P_2.

B. Experimental protocol and data processing

The experimental validation of the passive hip exoskeleton consisted of a 30-minute session. Ten healthy male subjects participated in the study selected through specific inclusion criteria. Subjects's anthropological characteristics are observed in Table I. Three levels of stiffness in the hip joint (i.e., low level - without pre-load, medium level - pre-load of 10N, and maximum level - pre-load of 15N). The participant was instructed to step onto a treadmill and perform the gait activity for 6 minutes at a fixed speed of 1km/h for each condition in the same order, as shown in Fig. 5. Two inertial sensors (Shimmer3 IMU Unit, Shimmer) were attached to the participant's feet at a sampling frequency of 128Hz to evaluate spatial-temporal parameters.

With this information, data processing was performed using MATLAB software (MathWorks, 2018b, USA) to filter the

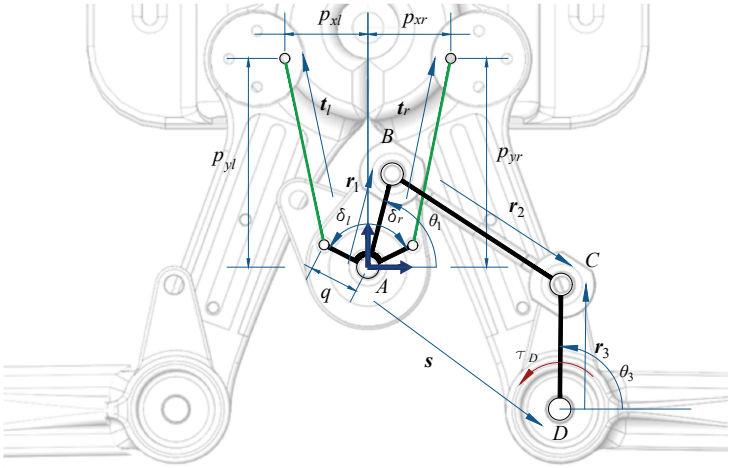

Fig. 4: Kinematic scheme of the hip mechanism

Algorithm 1 Kinematic and static solution's pseudo-algorithm.

$mech \leftarrow L_1, L_2, \theta_2, L_3, L_4$ ▷ Parameters of the mechanism.
$ROM \leftarrow 20°$ ▷ Hip ab/adduction range of motion.
$np \leftarrow 200$ ▷ Number of divisions within the ROM.
for $i \leftarrow PL_{min}$ **to** PL_{max} **do** ▷ Pre-load of composite tendons.
  for $j \leftarrow 0$ **to** np **do** ▷ Steps of 1.
    $\theta_3 \leftarrow$ KINEMATIC$(mech, \theta_2, ROM, j)$ ▷ Section II. B.1)
    $\tau_2, F_1, F_2 \leftarrow$ EXT. FORCES(θ_4, i) ▷ Section II. A.3)
    $\theta_2 \leftarrow \theta_2 + j \cdot (ROM/np)$
  return τ_2 ▷ Store each τ_2 per j

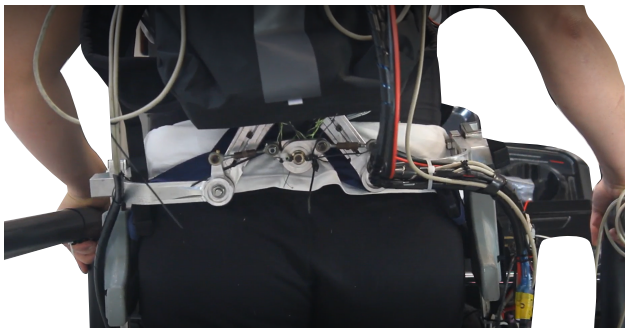

Fig. 5: Experimental test. Subject no. three is wearing the AGoRA lower-limb exoskeleton. The actuators of other planes were removed to analyse the influence of the hip joint along the frontal plane.

angular velocity of the right foot using a Moving Average Filter (MAF) with a 30ms window.

The SPSS software (IBM SPSS Software, USA) was used to identify significant changes in the three stiffness conditions: without stiffness (WOS), with 10N pre-load (WS10) and with 15N pre-load (WS15). Since the data had a normal distribution, a one-way ANOVA test was performed to find the p-value.

Characteristics	Mean ± SD
Age (years)	24.00 ± 2.00
Weight (kg)	75.60 ± 15.56
Height (cm)	175 ± 0.04
Hip Width (cm)	49.3 ± 2.79
Knee-Ankle Distance (cm)	39.7 ± 2.93

TABLE I: Mean and standard deviation of the characteristics of the ten subjects who participated in the study

C. Ethics Statement

The Research Ethics Committee of the Colombian School of Engineering Julio Garavito approved the protocol. All subjects have explained the procedure and purpose of the study and signed an informed consent form. They were allowed to leave the study at any time.

IV. RESULTS AND DISCUSSION

The proposed joint is studied following the aforementioned analytical approach and assessed through an experimental protocol. The first subsection aims to fully understand this joint, using the Algorithm 1 as a tool to assess the performance of the joint, varying two main features which are divided and presented into (1) the hip width variations allowed in the

AGoRA LLE and (2) the pre-load on the variable stiffness system. The second subsection presents the experimental results of the ten subjects, analyzing the phases for each leg.

A. Analytical results

Following the variation of the hip width that affects the joint's parameters, the analysis is aimed at five hip widths (i.e., 34 *cm*, 36 *cm*, 38 *cm*, 40 *cm*, 42 *cm*) to find the worst case scenario for the interaction torque (i.e., τ_D). Two main input variables are analyzed that influence these outcomes θ_3 and $p_{x\cdot}$ (the p_{xr} and p_{xl} variables are equally changed). The defined range of these input variables followed the hip ab/adduction ROM and design space available for θ_3 and $p_{x\cdot}$, respectively. The results also showed the force of each tendon (i.e., left tendon f_l and right tendon f_r) and the resultant torque produced by the composite tendons (i.e., τ_T).

The hip variation has a considerable effect on each variable, decreasing the magnitude of each one as the hip width increases. For instance, the magnitude of τ_D decreased by half only by increasing 8 *cm*. Similarly, the other variables were reduced by half their magnitude. The right tendon f_r mostly supports the motion in a range of -10 to 0 deg, delivering 150 to 0 N. In contrast, the left tendon f_l supports within a range of 0 to 10 deg, providing 0 to 200 N.

The variation caused by the hip width is related to the adjustable links, presented in Fig. 1, redefining the boundary conditions of the mechanism. In this sense, a greater hip width reduces the torque of interaction. Hence, the lack of energy to assist the user brings forth the need to pre-load the system.

Following, the system is analyzed along different pre-loads between 20 N to 140 N, considering the same input variables (i.e., θ_3, p_xl and p_xr).Moreover, this analysis is performed in the 42cm hip width scenario. The minimum pre-load increases τ_D by 120-240 times, providing a maximum torque interaction of 4.8 Nm, compared to the no-load scenario. In the maximum pre-load to the system, τ_D increases 4.25 times compared to the 20 N case. In contrast to the τ_T, which decreases between scenarios.

These kinetic capabilities are comparable to other hip joints presented in the literature. Using the outcomes of lower pre-load, the performance of the passive hip joint is greater than the torque interaction of XoSoft (i.e., maximum torque 3 Nm) [20]. Similarly, the hip exoskeleton studied by [18] provides 12 Nm less than the maximum pre-load scenario. However, the limitation of the passive hip joint is the pre-load adjustment. The magnitude applied to the joint relies on an instrument or mechanism. The current design adjusts the pre-load manually by using a lever arm on a rotational one-way clutch attached to the tendon. In this sense, the maximum pre-load can be problematic to achieve.

B. Experimental results

Table II shows the stance and swing times of the gait phases for each hip stiffness condition of the right foot. Table III shows the same information for the left foot. According to the statistical analysis, it is observed that there are no significant differences between the three conditions in both feet.

PHASES	WOS (s)	WS10 (s)	WS15 (s)	p-value
SWING	0.37 ± 0.07	0.39 ± 0.07	0.39 ± 0.08	0.79
STANCE	0.91 ± 0.17	0.90 ± 0.19	0.92 ± 0.23	0.97

TABLE II: Mean, standard deviation and p-value of swing and stance times of the gait cycle of the right foot. All data followed a normal distribution.

PHASES	WOS (s)	WS10 (s)	WS15 (s)	p-value
SWING	0.36 ± 0.07	0.34 ± 0.07	0.35 ± 0.08	0.91
STANCE	0.99 ± 0.17	1.00 ± 0.19	0.94 ± 0.23	0.76

TABLE III: Mean, standard deviation and p-value of swing and stance times of the gait cycle of the left foot. ll data followed a normal distribution.

After a stroke, patients with hemiplegia have a reduction in stability in the frontal plane, which affects their natural gait [24]; this is the reason why the experimental study suggests that limiting hip movement by increasing stiffness can generate stability that these patients do not have autonomously. Several exoskeletons have applied the principle of variable stiffness in different joints employing compliant actuators for safe human-robot interaction [25]. In the ankle, a compliant mechanism has been used to apply different stiffness levels to replicate the joint's range of motion during walking [26]. In the knee, this concept has been applied through a pneumatic artificial muscle (PAM), where different stiffness levels can be used to decrease muscle activity [27].

PHASES	WOS	WS10	WS15
SWING	0,44	0,94	0,76
STANCE	0,29	0,40	0,09

TABLE IV: p-values of the comparison between swing and stance times of a left and right foot.

Finally, in the hip this compliant principle has been found, however, they have been performed in the sagittal (anterior-posterior) plane, i.e., in hip flexion and extension. Zhou et al., using a passive exoskeleton with variable stiffness, found that muscle strength and activation decreased with increasing assistance and reduced the knee muscle's negative mechanical work [28]. Lee et al. have found that applying stiffness to the hip can influence kinematic changes in gait. As well as it does not change the symmetry between the two legs because it minimizes the net angular momentum generating stability [29]. This is confirmed in Table IV, showing no significant differences when comparing swing and stance times in the two legs when using the passive exoskeleton, altering the stiffness. This implies that the device does not alter the person's gait activity stability.

The hip abductors are essential for the function of the lower extremities and are part of the control of the mediolateral stability when standing [30]. In the experimental part of this study, the aim was to verify that the variable stiffness of the hip in abduction/adduction did not affect the spatiotemporal parameters in the anterior-posterior plane. Since the exoskeleton is intended to assist a patient with neurological diseases, its weight should not affect these gait parameters, meaning it should be kinematically compatible. This represents that the device does not affect the gait cycle phase times due to synchronization with the person's natural gait. Specifically, it

does not negatively affect the user's motor functions [31]. This indicates a potential use for future studies with pathological patients. However, future works can be performed with higher preloads to observe significant changes in the subject's gait and how this affects stability and spatiotemporal parameters.

V. CONCLUSIONS AND FUTURE WORKS

This work presents the design of a passive joint for the hip ab/adduction motion of the AGoRA exoskeleton. The mathematical principles were established and simulated to understand the capabilities of the passive joint. In addition, it also presented experimental results with different measures of hip stiffness in the mediolateral plane.

The analytical results present the interaction torque the passive joint produces, defining the necessity to apply a pre-load to the passive joint. On the other hand, experimental results show that there is stability in the three modes applied to the user. In addition, it is observed that the device does not affect the spatiotemporal parameters of gait in both legs, generating stability. However, future works can be aimed at the method of applying the pre-load in the passive joint to reach a higher magnitude, which also represents a higher interaction torque. Further work will also analyze the muscle activity in different hip stiffness.

REFERENCES

[1] W. H. Chang and Y.-H. Kim, "Robot-assisted Therapy in Stroke Rehabilitation," *Journal of Stroke*, vol. 15, no. 3, p. 174, 2013, ISSN: 2287-6391.

[2] D. Shi, W. Zhang, W. Zhang, *et al.*, "A Review on Lower Limb Rehabilitation Exoskeleton Robots," *Chinese Journal of Mechanical Engineering (English Edition)*, vol. 32, no. 1, 2019, ISSN: 21928258.

[3] K. H. Low, "Robot-assisted gait rehabilitation: From exoskeletons to gait systems," in *2011 Defense Science Research Conference and Expo (DSR)*, vol. 28, IEEE, Aug. 2011, pp. 1–10, ISBN: 978-1-4244-9276-3.

[4] G. Chen, C. K. Chan, Z. Guo, *et al.*, "A Review of Lower Extremity Assistive Robotic Exoskeletons in Rehabilitation Therapy," *Critical Reviews in Biomedical Engineering*, vol. 41, no. 4-5, pp. 343–363, 2013.

[5] S. Jezernik, G. Colombo, T. Keller, *et al.*, "Robotic Orthosis Lokomat: A Rehabilitation and Research Tool," *Neuromodulation: Technology at the Neural Interface*, vol. 6, no. 2, pp. 108–115, Apr. 2003.

[6] J. Meuleman, E. Van Asseldonk, G. Van Oort, *et al.*, "LOPES II - Design and Evaluation of an Admittance Controlled Gait Training Robot with Shadow-Leg Approach," *IEEE Transactions on Neural Systems and Rehabilitation Engineering*, vol. 24, no. 3, pp. 352–363, 2016.

[7] S. K. Banala, S. K. Agrawal, S. H. Kim, *et al.*, "Novel gait adaptation and neuromotor training results using an active leg exoskeleton," *IEEE/ASME Transactions on Mechatronics*, vol. 15, no. 2, pp. 216–225, 2010.

[8] K. A. Strausser, "Development of a Human Interface for a Wearable Exoskeleton for Users with Spinal Cord Injury," Ph.D. dissertation, 2011, p. 111.

[9] R. J. Farris, H. A. Quintero, and M. Goldfarb, "Preliminary Evaluation of a Powered Lower Limb Orthosis to Aid Walking in Paraplegic Individuals," *IEEE Transactions on Neural Systems and Rehabilitation Engineering*, vol. 19, no. 6, pp. 652–659, Dec. 2011.

[10] G. Zeilig, H. Weingarden, M. Zwecker, *et al.*, "Safety and tolerance of the ReWalk™ exoskeleton suit for ambulation by people with complete spinal cord injury: A pilot study," *Journal of Spinal Cord Medicine*, vol. 35, no. 2, pp. 96–101, 2012.

[11] J. Gancet, M. Ilzkovitz, G. Cheron, *et al.*, "MINDWALKER: a brain controlled lower limbs exoskeleton for rehabilitation. Potential applications to space," *11th Symposium on advanced space technologies in robotics and automation*, no. 1, pp. 12–14, 2011.

[12] H. Kawamoto and Y. Sankai, "Comfortable power assist control method for walking aid by HAL-3," *Proceedings of the IEEE International Conference on Systems, Man and Cybernetics*, vol. 4, pp. 447–452, 2002.

[13] N. Koceska and S. Koceski, "Review: Robot Devices for Gait Rehabilitation," *International Journal of Computer Applications*, vol. 62, no. 13, pp. 1–8, 2013.

[14] F. Leboeuf, J. Reay, R. Jones, *et al.*, "The effect on conventional gait model kinematics and kinetics of hip joint centre equations in adult healthy gait," *Journal of Biomechanics*, vol. 87, pp. 167–171, 2019, ISSN: 18732380.

[15] H. A. Quintero, R. J. Farris, and M. Goldfarb, "Control and implementation of a powered lower limb orthosis to aid walking in paraplegic individuals," in *2011 IEEE International Conference on Rehabilitation Robotics*, IEEE, Jun. 2011, pp. 1–6, ISBN: 978-1-4244-9862-8.

[16] V. L. Chiu, M. Raitor, and S. H. Collins, "Design of a hip exoskeleton with actuation in frontal and sagittal planes," *IEEE Transactions on Medical Robotics and Bionics*, vol. 3, no. 3, pp. 773–782, 2021.

[17] T. Zhang, M. Tran, and H. Huang, "Design and experimental verification of hip exoskeleton with balance capacities for walking assistance," *IEEE/ASME Transactions on mechatronics*, vol. 23, no. 1, pp. 274–285, 2018.

[18] J. Lee, K. Seo, B. Lim, *et al.*, "Effects of assistance timing on metabolic cost, assistance power, and gait parameters for a hip-type exoskeleton," in *2017 International Conference on Rehabilitation Robotics (ICORR)*, IEEE, Jul. 2017, pp. 498–504, ISBN: 978-1-5386-2296-4.

[19] T. Poliero, C. Di Natali, M. Sposito, *et al.*, "Soft wearable device for lower limb assistance: Assessment of an optimized energy efficient actuation prototype," *2018 IEEE International Conference on Soft Robotics, RoboSoft 2018*, pp. 559–564, 2018.

[20] C. Di Natali, T. Poliero, M. Sposito, *et al.*, "Design and Evaluation of a Soft Assistive Lower Limb Exoskeleton," *Robotica*, vol. 37, no. 12, pp. 2014–2034, 2019, ISSN: 14698668.

[21] M. Sanchez-Manchola, D. Gomez-Vargas, D. Casas-Bocanegra, *et al.*, "Development of a Robotic Lower-Limb Exoskeleton for Gait Rehabilitation: AGoRA Exoskeleton," in *2018 IEEE ANDESCON*, IEEE, Aug. 2018, pp. 1–6.

[22] B. Vanderborght, A. Albu-Schaeffer, A. Bicchi, *et al.*, "Variable impedance actuators: A review," *Robotics and Autonomous Systems*, vol. 61, no. 12, pp. 1601–1614, Dec. 2013.

[23] ASTM C1557-14, *Standard Test Method for Tensile Strength and Young's Modulus of Fibers*, West Conshohocken, PA, 2014.

[24] F. Januário, I. Campos, and C. Amaral, "Rehabilitation of postural stability in ataxic/hemiplegic patients after stroke," *Disability and rehabilitation*, vol. 32, no. 21, pp. 1775–1779, 2010.

[25] O. Baser, H. Kizilhan, and E. Kilic, "Employing variable impedance (stiffness/damping) hybrid actuators on lower limb exoskeleton robots for stable and safe walking trajectory tracking," *Journal of Mechanical Science and Technology*, vol. 34, no. 6, pp. 2597–2607, 2020.

[26] S. F. Abdulmajeed, K. S. Al-Kaabi, M. I. Awad, *et al.*, "Modeling, simulation and proof-of-concept of an augmentation ankle exoskeleton with a manually-selected variable stiffness mechanism," *Annals of Robotics and Automation*, vol. 4, no. 1, pp. 013–017, 2020.

[27] D. Maeda, K. Tominaga, T. Oku, *et al.*, "Muscle synergy analysis of human adaptation to a variable-stiffness exoskeleton: Human walk with a knee exoskeleton with pneumatic artificial muscles," in *2012 12th IEEE-RAS International Conference on Humanoid Robots (Humanoids 2012)*, IEEE, 2012, pp. 638–644.

[28] N. Zhou, Y. Liu, and Q. Song, "The effect of variable stiffness exoskeleton on the hip muscle groups during walking," in *2021 4th International Conference on Mechatronics, Robotics and Automation (ICMRA)*, IEEE, 2021, pp. 90–96.

[29] J. Lee, M. E. Huber, and N. Hogan, "Applying hip stiffness with an exoskeleton to compensate gait kinematics," *IEEE Transactions on Neural Systems and Rehabilitation Engineering*, vol. 29, pp. 2645–2654, 2021.

[30] D. A. Winter, F. Prince, J. S. Frank, *et al.*, "Unified theory regarding a/p and m/l balance in quiet stance," *Journal of neurophysiology*, vol. 75, no. 6, pp. 2334–2343, 1996.

[31] S. Ringhof, I. Patzer, J. Beil, *et al.*, "Does a passive unilateral lower limb exoskeleton affect human static and dynamic balance control?" *Frontiers in Sports and Active Living*, p. 22, 2019.